Thermal management system of LNEG pilot area: numerical analysis and experimental validation

Volodymyr Pobuta
volodymyr.pobuta@tecnico.ulisboa.pt

Instituto Superior Técnico, Universidade de Lisboa, Portugal

May 2023

Abstract

Buildings contain 30% of final energy consumption worldwide, representing a big opportunity in the fight for decarbonization of the economy. The IMPROVEMENT project is part of European efforts to fight climate change and has the task to study the integration of RES systems in public buildings, with high power quality and thermal comfort. The Portuguese pilot plant was retrofitted to a thermal-power microgrid to achieve these goals.

This work focused on analyzing experimental data and creating a numerical model in TRNSYS to extrapolate for longer periods of time. The processed experimental data shows great promise of a working power micro-grid, but results are less promising when talking about a thermal micro-grid. Energy management is crucial to avoid energy losses in "idle" equipment, as well as to minimize energy consumption through consistent monitoring. Behavioural change in users is necessary to operate the system at more optimal points.

Keywords: Nearly Zero Energy Buildings, Energy Efficiency, Key Performance Indicators, Micro-grid, Energy Management System, Thermal Management System

1. Introduction

As of 2021, the buildings sector accounts for 30% of the world´s GHG emissions and energy consumption [5]. To tackle the energy crisis of the 21^{st} century and the challenges of climate change, it is important to introduce massive changes in each of society´s fundamental sectors in order to mitigate the damage.

In Europe, the impact of the buildings sector is even higher than the global average, reaching a value of around 40%, in which the biggest contributors are space and water heating [7]. Despite having a steep increase in renewable implementation and investment, most of Europés energy is still imported from countries like Russia, which is comprised of mostly fossil fuels like natural gas and oil [2].

To mitigate this dependency on non-RES sources of primary energy in buildings, it is important to investigate the possibility of integration of RES sources in buildings. The goal of the SUDOE IMPROVEMENT project is to investigate the integration of these sources of energy in public buildings, aiming to achieve isolated micro-grids, capable of producing its own thermal and electric energy.

2. Background

In 2019, LNEG entered the SUDOE IMPROVEMENT project and a decision was made to create an experimental pilot area in Building C of Lumiar Campus. The goal was to create an isolated electric micro-grid, capable of supplying enough electrical power to meet the demand of the pilot area equipment, as well as a ventilation system with an auxiliary solar collector sub-system integrated, which could complement some of the thermal demand during the heating season [3].

2.1. Location of pilot area

The LNEG Campus is located in Lisbon, as seen in Figure 1, in an area with a mean annual irradiation of $1750 W/m^2$ [1]. Building C, in which the pilot area is located, was built in the decade of 1960, in a time when building design did not include any of the efficiency guidelines which are obligatory nowadays.

Room	Functionality	Area (m^2)	Volume (m^3)
1052	Conference room	83.4	225.29
1054	Meeting room	22.1	66.27
1050	Office	10.8	32.43
1051	Office	10.8	32.43

Table 1: Areas and volumes of monitored pilot plant rooms

The pilot area belongs to the ground floor of the buildings C, to the left of the main entrance of the building, as seen in Figure 2. It is composed of three offices, one small meeting room, one larger conference room and a connecting corridor, with a floor surface area of around 140 m^2 (detailed areas and volumes of each of ventilated and monitored areas are in Table 1).

Figure 1: Google Maps location of LNEG Campus in Lumiar

2.2. Renovations

The pilot area suffered some minor renovations - new panels with high acustic and thermal insulation replaced the old pasterboard panels from the fake ceiling, while an airbox was installed on the E and W walls.

Figure 2: Bird-view of Building C plant, with the pilot area highlighted

3. Numerical model in TRNSYS

To study the performance of the installation, a numerical model was created in TRNSYS software. The building model was created with a special plug in called TRNBUILD, which connects itself to the main simulation evironment of TRNSYS by the Type 56 [6]. In Table **??**, a detailed description is presented of all the wall layers used in the model, with the mean heat loss coefficient for each of them.

To model the windows, a . While the real windows have a U of around 2.68, the closest TRNSYS model had a value of 2.85.

The next steps were to indicate the gains of the pilot area and the working schedule of each of the rooms. The gains from people was adjusted according to the $EN13779$ norm for stationary activity in an office, for the mean air temperature of 24^oC. For each person occupying any of the rooms, an additional gain of equipment will be associated, which will correspond to the personal computer each person is using. As for the light, the gains were made equivalent to an LED lightning fixture, each each with a power rating of $75W$. These gains are summarized in Table 2, while the occupancy schedules are presented in Figures 3, 4 and 5.

Gain	Convective (W)	Radiative (W)
People	37.5	37.5
Lightning	46.11	11.67
Equipment	25	25

Table 2: Summary of internal gains defined for pilot area

The infiltration rate was computed according to ASHRAE HOF Chapter 16, which sets this value at 5.4 m^3 /h m^2. Replacing the variables with the values of the geometrical model, a value of 0.6 was

used in each of the rooms of the pilot area. Other properties, such as air and humidity capacitance, which relate to the capacity of air, humidity and furniture to absorb and dissipate energy, were set at 5 and 10 times the pre-defined values, accordingly - this multipliers came from TRNSYS manuals.

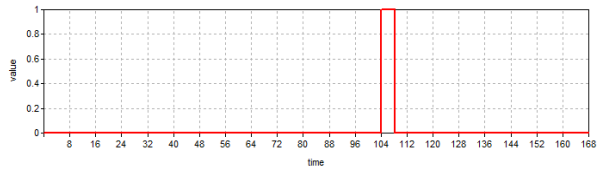

Figure 3: Occupancy schedule of room 1052 (conference room)

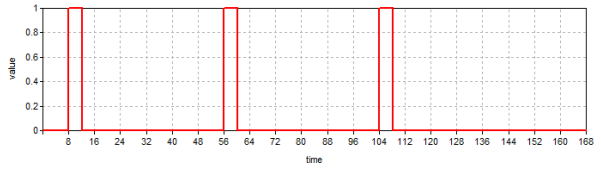

Figure 4: Occupancy schedule of room 1054 (meeting room)

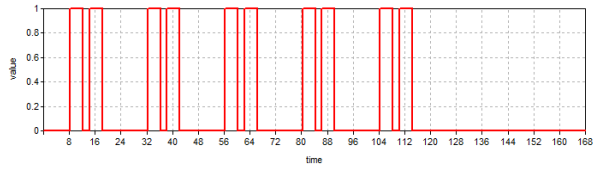

Figure 5: Occupancy schedule of room 1050 (personal office)

3.1. Climatization Modelling

The modelling of the active systems of the installation followed the passive part of the pilot area. The climatization system can be decomposed in 4 subsystems, which are connected to the central storage tank of 1000L. The components of each of these subsystems is shown in Table 3, as well as the corresponding Types in the TRNSYS environment.

To simulate the operation of the pilot area equipment, the following schedules were defined for each of the subsystems:

1. Heat pump - Monday to Friday, from 8:00 to 20:00
2. Fan coil circulation pump - Monday to Friday, from 8:00 to 20:00
3. Renovation circuit - Monday to Friday, from 9:00 to 12:00 and from 13:00 to 18:00
4. Solar system - Monday to Sunday, from 10:00 to 17:00

Subsystem	Component	TRNSYS Type
Solar	Primary pump	Type 114 - Single speed pump
	Secondary pump	Type 114 - Single speed pump
	Solar tank	Type 156 - Cylindrical Storage Tank with immersed heat exchanger
Heat pump	Heat pump	Type 941 - Air-to-Water Heat Pump
	Circulation pump (internal)	Type 114 - Single speed pump
Climatization	Fan coils	Type 600 - 2-Pipe Fan coil (adjusted for each model)
	Circulation pump	Type 114 - Single speed pump
Air renovation	Heat exchanger	Type 760 - Sensible Air-to-Air Heat Recovery with Controlled Outlet Conditions
	Fans	Type 146 - Single speed fan

Table 3: List of key components of LNEG pilot area thermal system and the TRNSYS counterparts

The solar system is composed of a primary circuit and secondary circuit. The primary one is controlled according to the outlet temperature of the collectors, T_{out}^{coll}, and the mean temperature of the solar tank, T_{solar}, while the secondary circuit takes into consideration the same mean temperature of the solar tank, the mean and outlet temperature of the inertial tank, $T_{inertia}$ and $T_{inertia}^{out}$ respectively. The primary circuit has a safety condition to avoid the build up of extremely high temperatures, while the secondary one focuses on the setpoint temperature of the inertial tank, $T_{inertia}^{setpoint}$.

$$T_{out}^{coll} - T_{solar} > 1 \wedge T_{solar} < 80 \quad (1)$$

$$T_{solar}^{out} - T_{inertia} > 1 \wedge T_{inertia}^{out} < T_{inertia}^{setpoint} \quad (2)$$

The heat pump components work simultaneously with the same control strategy, which changes according to the season.

$$T_{out}^{inertia} < T_{setpoint}^{heating} - 1 \quad (3)$$

$$T_{out}^{inertia} > T_{setpoint}^{cooling} + 1 \quad (4)$$

$$C_{pump} = C_{hp}^{heating} + C_{hp}^{cooling} \quad (5)$$

Equations 3 and 4 represents the moment at which the heat pump is enabled, while the control for the circulation pump is represented by equation 5 - it activates whether the system is in cooling or heating mode ($C_{hp}^{heating}$ and $C_{hp}^{cooling}$ are the representative variables for the heating and cooling control of the heat pump).

As for the fan-coils, the chosen operation mode was "Auto", which required a fine control depending on the differential between the room and setpoint temperature. Depending on the season, the control strategies will change.

To validate the numerical model, the MBE and $cvRMSE$ statistical parameters were used to verify if it represented the pilot area accurately [4]. The validation was done for the period before and after the renovations, in the cooling and heating seasons. Metheorological data gathered on site of the LNEG Campus was used as an input for the simulation program and the experimental and simulation results for the air temperature were used for the validation.

In the case of active systems in operation, the statistical indicators fell in the acceptable range to accept the model as being validated (for an hourly calibration, ±10% for NMBE and ±30% for cvRMSE). As seen by Figures 6 and 7, the simulated and experimental results fall very close one to the other. For the heating season, the time period chosen was from 16th to 22nd of January and for the cooling season it was from 11th to 17th of July.

As seen by Tables 4 and 5, the statistical indicators fall withing the acceptable range, thus validating the model. This allows to extrapolate the results for longer periods of time with confidence that the results will follow any experimental measurements.

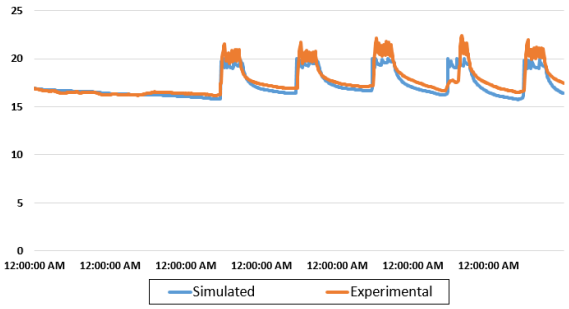

Figure 6: Validation results from heating season with active systems on, room 1054

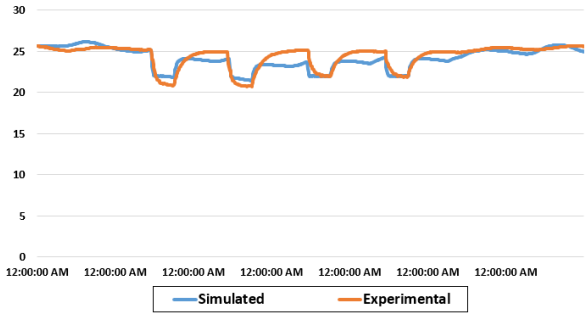

Figure 7: Validation results from cooling season with active systems on

4. Experimental Results

4.1. Passive solutions

To evaluate the effectiveness of the passive solutions after the renovations took place, an analysis was made for the heating and cooling season separately. To better adjust the results, two periods of time with similar metheorological conditions had to be chosen, considering they are located in different years. Due to the difficulty of finding sequential periods in both the years of study, which could meet these conditions, the results will be affected by the inertial effects of the building.

To quantify the improvements that these solutions gave to the thermal performance of the pilot area, Equation 6, which calculates an approximate amount of energy necessary to heat/cool the air inside the room to a certain setpoint temperature - in winter, this setpoint was set at 20 degrees, while in summer it was left at 24.

$$Q_{thermal} = m\ C_p\ \Delta T\ = \rho\ V\ C_p\ (T_{setpoint} - T_{air}) \quad (6)$$

	11-Jul	12-Jul	13-Jul	14-Jul	15-Jul	16-Jul	17-Jul
MBE	0.5%	-0.6%	-1.8%	-1.7%	-2.6%	-1.5%	-3.4%
RMSE	0.13	0.21	0.68	0.72	0.91	1.08	1.08
A	25.35	23.75	23.38	24.00	24.00	25.10	25.42
cvRMSE	0.5%	0.9%	2.9%	3.0%	3.8%	4.3%	4.3%

Table 4: Statistical indicators of the validation of heating season with active systems, room 1054

	11-Jul	12-Jul	13-Jul	14-Jul	15-Jul	16-Jul	17-Jul
MBE	1.7%	0.7%	-1.2%	-4.1%	-2.9%	-2.0%	-0.8%
RMSE	0.51	0.60	0.84	1.24	0.90	0.63	0.39
A	25.35	23.75	23.38	24.00	24.00	25.10	25.42
cvRMSE	2.0%	2.5%	3.6%	5.2%	3.8%	2.5%	1.5%

Table 5: Statistical indicators of the validation of cooling season with active systems, room 1054

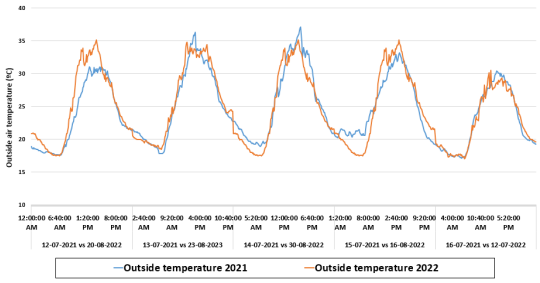

Figure 8: Outside air temperature in 2021 and 2022 in cooling season

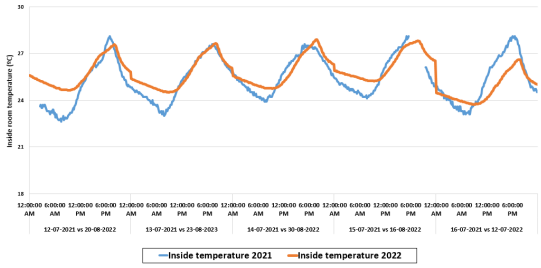

Figure 9: Inside air temperature in 2021 and 2022 in cooling season

The period of time chosen for the cooling season was from the 12th to 16th of July in 2021 and in 2022 the corresponding days were chosen: 20th, 23rd, 30th, 16th of August and 12th of July - as seen in Figures 8 and 9. As for the heating season, in 2021 6th and 15th of March were chosen, with 19th and 26th as counterparts in 2022 - as seen in Figures 10 and 10. Not only was it hard to find similar metheorological conditions in the rooms, but similar occupancy schedules as well, which led to the choice of non-sequential periods of time. The effect of thermal inertia of the building will be felt for this exact reason.

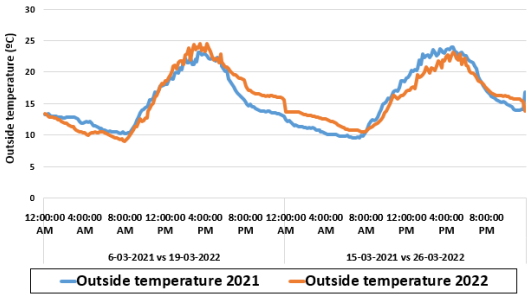

Figure 10: Outside air temperature in 2021 and 2022 in heating season

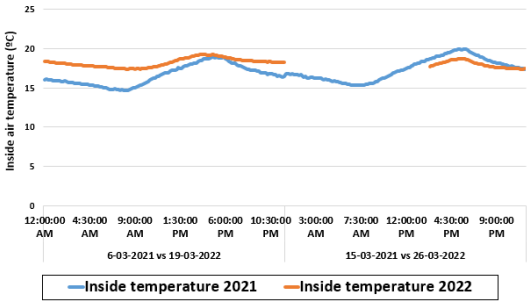

Figure 11: Inside air temperature in 2021 and 2022 in heating season

For the cooling season, the energy demand after renovations took place was around 16%, while in the heating season the renovations had a more profound impact, reaching a value of 23%.

4.2. Active solutions

The data gathered from the monitoring of the electrical system was used to evaluate how well the pilot area adjusts to the nZeb philosophy.

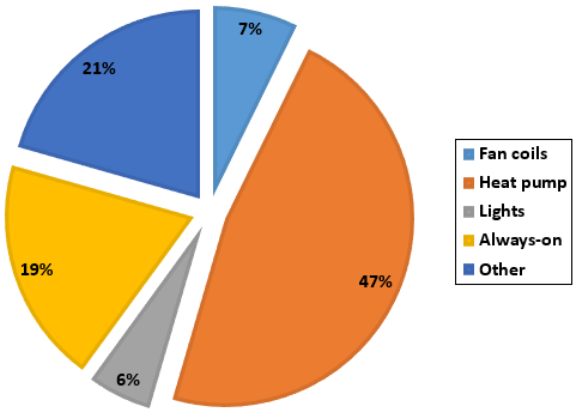

Figure 12: Yearly consumption percentage

As seen in Figure 12, the heat pump is the equipment with the biggest contribution of energy consumption, however, a big percentage belongs to equipments "Always on" and others, which include all the sensors and controllers. This could be explained by big periods of time of equipments in "idle" mode, when neither the heat pump or the fan-coils were working and thus the whole energy consumption came from these parasitic sources.

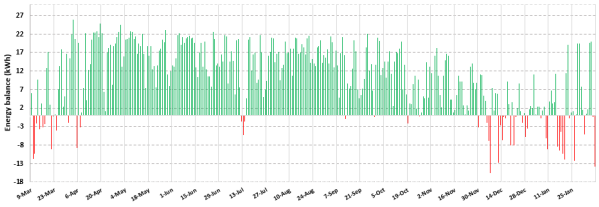

Figure 13: Surplus and shortage of production from February 2022 until March 2023

By looking at Figure 13, most of the year the production exceeded the consumption by large amounts. However, there is a constant load, which could be represented by idle equipment and controllers, alongside a very regular curve of consumption which can only represent the consumption in the room 1048 - as seen in Figure 14. On certain occasions, the consumption rose drastically - for example, in summer during project meeting and conferences and in winter during regular testing of the equipment - which then puts the surplus in the red zone.

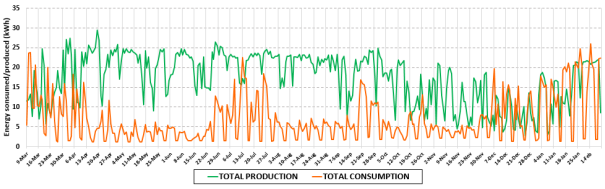

Figure 14: Total production and consumption from February 2022 until March 2023

The comparison between the direct and economic modes is also important to verify the advantage that the economic configuration gives in relation to the more traditional one. As such, two periods of time with similar metheorological conditions were chosen to compare both modes of operation. Due to unavailability of data for proper analysis of the heating period, only data for the cooling period will be analysed.

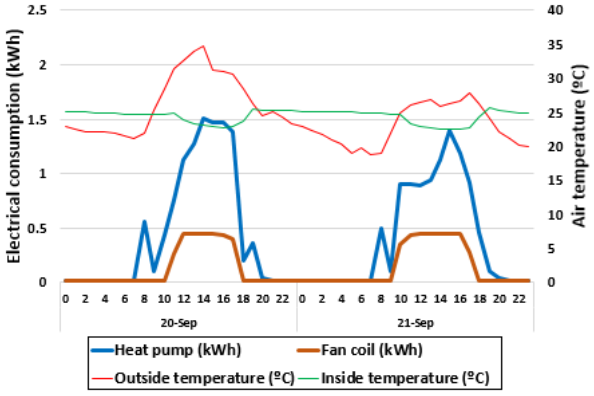

Figure 15: Consumption of heat pump and fan coils in direct mode, 20th an 21st of September

Figure 15 shows a typical consumption profile for the direct mode, which differs from Figure 16 by the initial peak of consumption, explained by the difference in mixture tank volumes. Although in both these periods the occupancy schedule is similar and the metheorological conditions match closely, the energy savings for the economic mode are minimal, reaching a value of 2.3%. Although the improvements might seem minimal, it must be pointed out that in cooling mode the system also receives a lot of energy from the photovoltaic panels, which could lead to 100% RES supplies thermal and electrical energy.

5. Simulation Results

Several simulation were performed in order to access the performance of the pilot area installation with

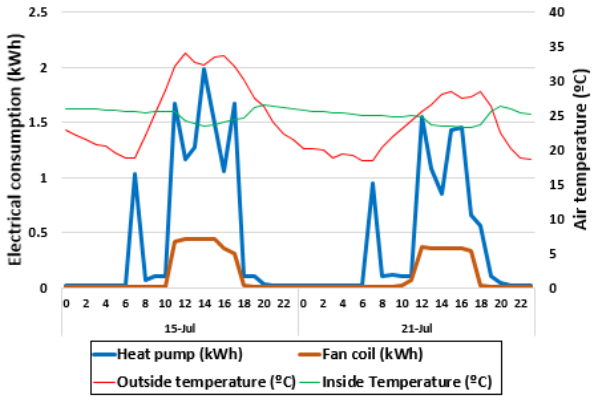

Figure 16: Consumption of heat pump and fan coils in economic mode, 15th and 23rd of July

different configurations. The performance was analysed by the Key Performance Indicators, or KPI´s, which involved both the electric/thermal installation as well as comfort indicators inside of the pilot area. The variables chosen for this parametric study were:

1. Volume of inertial tank - 600, 1000 and 1500 L were the volumes chosen, all related to tanks from the same series as for the installed model. To better adjust the simulation results, the height of the tanks was introduced as an auxiliary variable, $H_{inertia}$ (accordingly, $H_{inertia} = [1.73 \ ; \ 2.25 \ ; \ 2.32]$)

2. Setpoint temperature of inertial tank - Depending on the season, different setpoint temperatures for the inertial tank had to be chosen. For winter, the range was [40; 43; 45; 47; 50] and for summer [8; 10; 12; 14; 16]

3. Room setpoint temperature - The setpoint temperature also changed according to the season - for winter the range was [18; 19; 20; 21; 22] and for summer [21; 22; 23; 24; 25]

5.1. Thermal energy savings

Thermal Energy Savings shows the variation in thermal energy required to heat/cool the pilot area - in the respective seasons - compared to a reference case, which was chosen to be the pilot area before the renovations took place.

$$TES(\%) = \left(1 - \frac{E_i}{E_{ref}}\right) \times 100 \qquad (7)$$

E_{ref} represents the energy required to heat/cool the space for the reference case, while E_i represents all the case studies presented in the following list:

1. Reference case (meaning that TES = 0)

2. Renovated pilot area

3. Renovated pilot area with better windows

4. Renovated pilot area, with better windows and 10cm woolrock insulation on E and W walls

5. Renovated area, with better windows, 10cm woolrock insulation on E and W walls and infiltration rate equal to a "passive house"

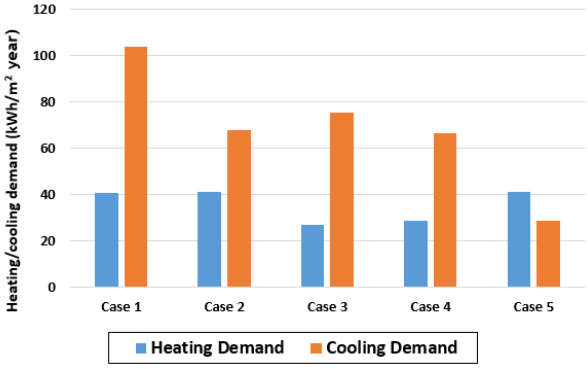

Figure 17: Thermal Energy Savings for the 5 case studies presented

Figure 17 shows the effect of the increased quality of possible passive solutions in the pilot area. As the quality increases, more energy can be saved during the heating period, as the internal gains contribute to aleviate the heating demand of the space, while the passive solutions avoid at maximum any energy exchange between the interior and exterior. As for the cooling period, the inverse behaviour can be seen, which can be explained by the negative effect of internal gains on the energy balance of the room, as the increased quality of renovations creates a greenhouse effect inside of the room, thus increasing the cooling needs during hot days.

5.2. Solar fraction

$$f_{solar} = \frac{Q_{HX}}{Q_{HX} + Q_{HP}} \qquad (8)$$

Q_{HP} represents the energy supplied by the heat pump to maintain the setpoint temperature of the inertial tank at the setpoint, while Q_{HX} relates to the energy transfered from the solar tank to the inertial tank through the heat exchanger.

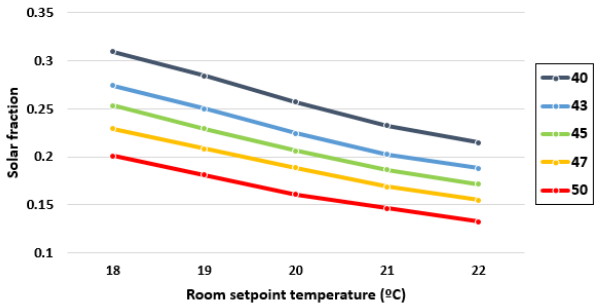

Figure 18: Solar fraction for $V = 600L$

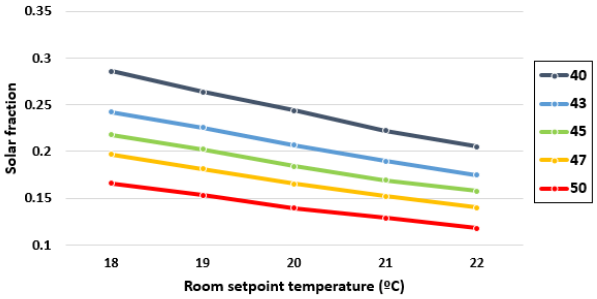

Figure 19: Solar fraction for $V = 1000L$

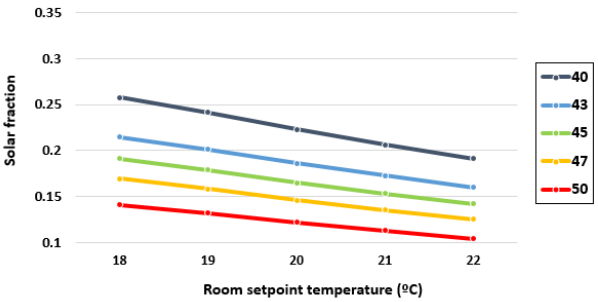

Figure 20: Solar fraction for $V = 1500L$

With the increase in volume, inertial tank and room setpoint temperatures, the solar fraction decreases, as seen in Figures 18, 19 and 20. The increase in the value of these variables increases also the energy required to maintain the inertial setpoint temperature, so a lower volume is preferable when trying to maximixe the thermal solar gain.

5.3. SCOP Seasonal Coefficient of Performace

$$SCOP = \frac{Q_{SH}}{E_{SH}} = \frac{Q_{HP} + Q_{HX}}{E_{pump}^{solar} + E_{HP}} \tag{9}$$

The definition of SCOP says that it is the fraction of heat supplied by the energy consumed. The heat supplied is a sum of the solar contribution, Q_{HX} with the heat pump delivered energy, Q_{HP}. As for energy supplied to operate this subsystem, the solar pumps (primary and secondary), E_{pump}^{solar} and the heat pump E_{HP} electric consumption is included.

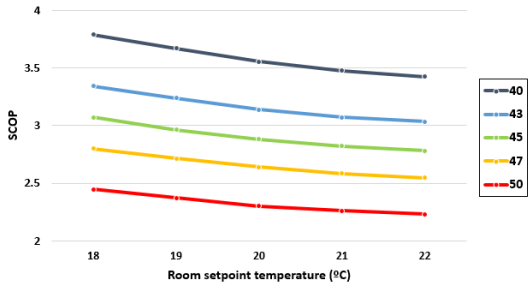

Figure 21: Seasonal Coefficient of Performance for $V = 600L$

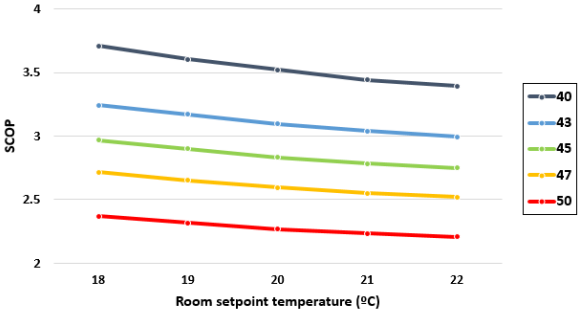

Figure 22: Seasonal Coefficient of Performance for $V = 1000L$

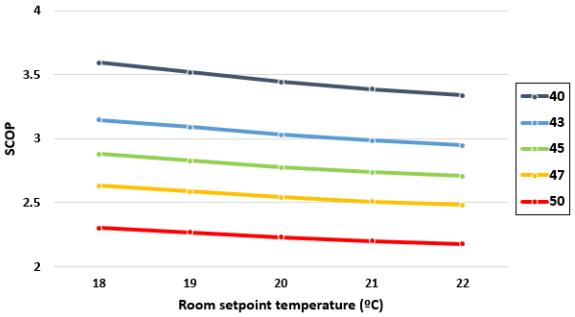

Figure 23: Seasonal Coefficient of Performance for $V = 1500L$

The behaviour of SCOP is similar to the solar fraction - as the heating demand increases by the means of volume and setpoint temperature increase, more electrical power is required to supply the energy necessary to maintain a steady setpoint temperature in the inertial tank. Also, for lower volumes, more heat is delivered by the collectors,

which consumes much less energy than operating the heat pump. This relations can be seen in Figures 21, 22 and 23.

5.4. SEER

The definition of SEER is similar to SCOP, however the energy demand comes in the form of cooling. As there are no "free" sources of cooling energy, this KPI will only take into consideration the energy output of the heat pump, Q_{HP}, divided by its electric consumption, E_{HP}.

Looking at Figures 24, 25 and 26, no significant change can be associated with the increase of volume or room setpoint temperature. However, when changing the setpoint temperature of the inertial tank, the efficiency of the system in cooling mode increases. As the heat pump operates with inlet water coming from the inertial tank, the lower the difference in water coming into the heat pump and out of it, the more efficiently it operates. By changing the setpoint temperature, there is less difference between the temperature of the water and the room temperature, so the water increases the temperature more slowly.

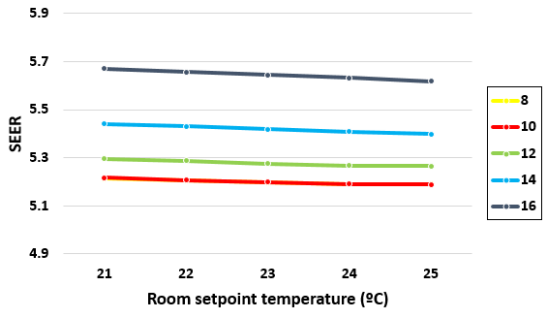

Figure 24: Seasonal Energy Efficiency Ratio for $V = 600L$

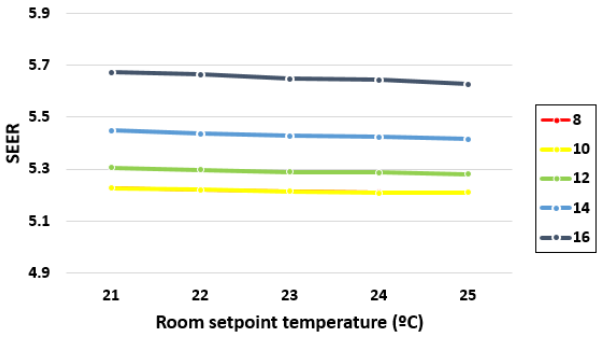

Figure 25: Seasonal Energy Efficiency Ratio for $V = 1000L$

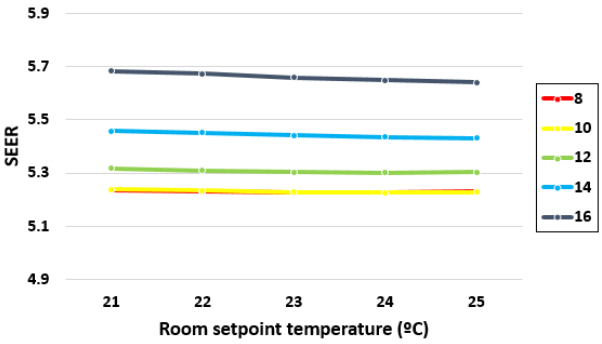

Figure 26: Seasonal Energy Efficiency Ratio for $V = 1500L$

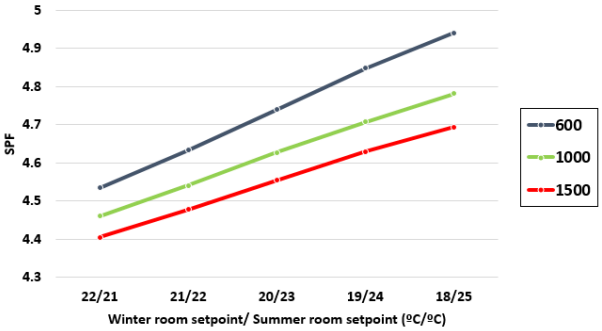

Figure 27: Seasonal Performance Coefficient for $V = 600, 1000$ and $1500L$

5.5. SPF

SPF is a combination of both the previous KPI´s, showing the performace of the system all though the year. The delivered thermal energy includes the energy delivered by the heat pump in cooling and heating mode, as well as the energy delivered by the collectors. As for the energy supplied, all the contributions are included, for heating and cooling season.

Due to the large number of variables, a simpler form of analyzing this KPI was created. The *x-axis* represents the room setpoint temperatures, for heating and cooling season, in decrescent order of the differential between the said temperature and the mean ambient temperature.

Figure 27 shows that the yearly performance of the system increases as the room setpoint approaches the mean ambient temperature. As this differential comes closer to zero, the need for cooling or heating decreases drastically. Especially during winter, if the setpoint temperature is lowered enough, the internal gains have a massive effect on thermal demand reduction.

6. Conclusions

Despite the difficulty in gathering enough experimental data from the pilot area, some conclusions

were taken about the work done:

1. The passive solution improved thermal behaviour of the inside air temperature, either in heating or cooling season, reducing thermal demand in 23% and 16% respectively

2. If the climatization system is not being actively used, a lot of energy is lost in "idle" operation, such as controllers and "always-on" equipment.

3. In similar metheorological conditions during the cooling season, the economic mode has little difference between the direct one in cooling mode

4. The contribution of the solar system during heating season is very low, at around 11 % of total thermal energy needs

When it comes to results from the numerical model, some major conclusions can be taken:

1. The increase of quality of passive solutions has a positive effect during the heating season, however it can have a negative effect during cooling season, as it can create a sort of "greenhouse" effect inside of the room

2. Solar fraction and SCOP improve with the decrease of inertial tank volume and setpoint tempeture, as well as with room setpoint temperature.

3. During cooling season, the performace only increases with the increase of the inertial tank setpoint, while being practically unchanged regarding the other two variables

4. The yearly performance of the system can be improved with the decrease of the differential between the room setpoint temperature and the mean ambient temperature, as well as of the inertial tank volume.

Acknowledgements
The author would like to thank the team from LNEG, mainly Jorge Facão, David Loureiro and João Correia, in the support given and all the absorbed experience from participating in such an important and internationally renowned project. An honorable mention goes to Dr. Carlos Silva from IST, which coordinated and supported the elaboration of this work.

References

[1] A. Cavaco, H. Silva, P. Canhoto, S. Neves, J. Neto, and M. Collares Pereira. Annual average value of solar radiation and its variability in portugal. 2016.

[2] E. E. Commission). Energy, transport and environment statistics, 2020.

[3] A. Estanqueiro, A. Joyce, L. E. Aelenei, J. Facão, C. Rodrigues, D. Loureiro, J. Teixeira, J. B. Correia, Á. Ramalho, S. Camelo, et al. Conversão de edifícios existentes em nZeb através da integração de energias renováveis, de micro-redes e de soluções de eficiência energética. In *CIES2020-XVII Congresso Ibérico e XIII Congresso Ibero-americano de Energia Solar*, pages 987–995. LNEG-Laboratório Nacional de Energia e Geologia, 2020.

[4] E. Fabrizio and V. Monetti. Methodologies and advancements in the calibration ofbuilding energy models.

[5] I.E.A. World energy outlook 2022, IEA, Paris https://www.iea.org/reports/world-energy-outlook-2022, License: CC by 4.0 (report). *CC BY NC SA*, 4.0. Annex A.

[6] M. Rashad, A. Żabnieńska-Góra, L. Norman, and H. Jouhara. Analysis of energy demand in a residential building using TRNSYS. *Energy*, 254:124357, 2022.

[7] T. Wilberforce, A. Olabi, E. T. Sayed, K. Elsaid, H. M. Maghrabie, and M. A. Abdelkareem. A review on zero energy buildings–Pros and Cons. *Energy and Built Environment*, 4(1):25–38, 2023.